Iran J Public Health, Vol. 45, No.5, May 2016, pp.657-669

Original Article

A Model for Diagnosing Breast Cancerous Tissue from Thermal Images Using Active Contour and Lyapunov Exponent

Hossein GHAYOUMI ZADEH, Javad HADDADNIA, Alimohammad MONTAZERI

Dept. of Biomedical Engineering, Hakim Sabzevari University, Sabzevar, Iran

***Corresponding Author:** Email: h.ghayoumizadeh@gmail.com

(Received 23 Jun 2015; accepted 16 Dec 2015)

Abstract

Background: The segmentation of cancerous areas in breast images is important for the early detection of disease. Thermal imaging has advantages, such as being non-invasive, non-radiation, passive, quick, painless, inexpensive, and non-contact. Imaging technique is the focus of this research.

Methods: The proposed model in this paper is a combination of surf and corners that are very resistant. Obtained features are resistant to changes in rotation and revolution then with the help of active contours, this feature has been used for segmenting cancerous areas.

Results: Comparing the obtained results from the proposed method and mammogram show that proposed method is Accurate and appropriate. Benign and malignance of segmented areas are detected by Lyapunov exponent. Values obtained include TP=91.31%, FN=8.69%, FP=7.26%.

Conclusion: The proposed method can classify those abnormally segmented areas of the breast, to the Benign and malignant cancer.

Keyword: Breast cancer, Surf and sift algorithm, Active contour, Thermography

Introduction

Breast disease is one of the major issues in women's health today. Early detection of breast cancer is important in reducing mortality rates. Early detection and eradication of malignant tumors at an early stage before metastasize and spread to neighboring areas, can be prevented from threats and problems later. During 2003-2007, the median age of death from breast cancer has been 68 yr. Almost 0.0%, 0.9%, 6.0%, 15.0%, 20.8%, 19.7%, 22.6% and 15.1% of mortality has occurred in the following order, 20 yr, 20-34, 35-44, 45-54, 55-64, 65-74, 75-84 and above 85 yr(1). Report submitted shows that 0% detection has been possible in those under the age of 20. While 1.9%, 10.2%, 22.6%, 24.4%, 19.7%, 15.5% and 5.6% of diagnosis has been possible in the inside groups ranging , 34-44, 45-54, 55-64, 65-74, 75-84 and above 85 yr (1). Early detection can lead to 85 percent chance of survival (2).

Early detection of breast cancer is one of the most important issues that researchers have always sought. Pathological mechanism of breast cancer is formed in this manner while cancerous cells produce nitric oxide (no) in the proliferative phase (proliferative). The chemicals cause difficulties in neural control, and thus lead to regional artery dilatation in the early stages of cancer cells growth. This angiogenesis causes increment in the local temperature even a few years earlier than tumor formation. Deep lesions can cause changes in skin temperature (3, 4). Based on the features listed above, this concept means that, some features used in the diagnosis of breast cancer, entail geometric size, location, shape, topology as well as the thermal features.

Because, doctors are interested in the thermal imaging after a long time, which comprise the following: 1) progress done in the technology of infrared cameras; 2) creation of standard rules for thermal imaging; 3) accurate calibration of the camera. Breast Thermography is a potential technique with useful protocol (5), which has advantages such as non-invasive, non-radiation, passive, quick, painless, inexpensive, and non-contact camera (6-11). Breast Thermography is suitable for women of all ages, including pregnant and nursing women and women with dense tissue in their breast (12). Thermography is the measurement of published heat from different parts of the human body**.** Infrared imaging is a non-invasive method adopted as a diagnostic tool (13). Thermogram of a patient provides the distribution of heat in the body. Due to the high metabolic rate and progression of vascular angiogenesis, the cancer cells have a higher temperature than the normal cells around them. Thus, cancer cells in infrared images can be indicated in the form of critical focus. Thermography is better than the method of mammography in predicting breast cancer in its early stages, even when the tumor is at the initial stage of formation. Medical Thermography has become a tool for early warning. Thermal imaging has been used for diagnosis of breast cancer. The effect of early detection is not within the scope of this paper. Techniques and image processing algorithms are the problems of medical applications.

One of concerns related to algorithms choice is sensitivity and accuracy. Medical thermography could not progress for a long time because of the dependency on hardware and software fields and limitations concerning existing. Recently hardware limitations have declined with the improvements made in the field of photo detectors and PCs. Limitation of software decreased with the progress made in the analysis of algorithms. All the items listed, indicate the success related to the use of thermal images in medicine (5). Recently, case studies have been implemented on breast cancer detection in large-scale by thermal imaging, mostly indicate average sensitivity and specificity of 90% (7). Parametric analysis is not solved in abnormal areas that are hot and cold points. Thermal imaging is employed in diverse medical applications such as breast cancer detection (14), pain management (15), and diabetes (16). Methods are proposed for the analysis of image processing algorithms such as abnormal statistical methods, thermal asymmetric methods and descriptive matching (17-19). Although the image processing techniques are important for the analysis of medical thermography, many of these methods are not sensitive enough or delicate algorithms are not applied extensively for independent detection by using of computer. The purpose of this paper is to provide a diagnostic tool by using computer based on thermal model (7). One of the primary problems for the clustering and detecting breast cancer in thermal imaging is that both of breast areas must first be segmented so that the image processing be performed on it (20). Since thermal images have diverse formats (small or large, condensation, etc.), separating special area whit high accuracy is very difficult. On the other hand, the extracted area is not accurate enough for the next step. Some papers (21) have used asymmetry of the two regions and moments. In the proposed method, the problem has been fixed and there is no requirement to separate the breast from the beginning. Identification of the correct boundary and image segmentation is one of the most important issues in the utilization of machine vision applications, such as traffic monitoring in urban transport systems (22, 23), medical applications (24), video monitoring and target identification in air defense weapons (25). One problem in computer analysis of the thermal images is that the images should be obtained directly from the patient to avoid encountering with the problems during the analysis of such asymmetry. The method is presented so as to detect early breast cancer in rotated images.

It is difficult to separate cancerous tissue in thermal images; the goal of this paper is to solve this problem. The proposed models are the combination of SURF and SIFT which are related to feature extraction. Active contour has been used in the first phase. Whit regard to computer vision; contour models describe the boundaries of shapes within an image. Few papers are in the field of thermography have used active contour method to separate but these are not pertinent to breast cancer. Active contour method has been adopted for segmenting masses

on Breast ultrasound images (26). Active contour model has been presented for Breast Contour Detection (27). Previous models were not related to infrared image within the scope of breast cancer. And finally in the proposed method, Lyapunov exponent has been used for detecting benign and malignant cancer. Lyapunov exponents are quantities that characterize the average rate of divergence or convergence of two neighboring trajectories in the PS. It can measure the sensitive dependency on the initial conditions (28).

Materials and Methods

The proposed method requires that body organs in the thermal image be separated into distinct parts**.** For this purpose, firstly, Limb skeleton study must be segmented from the thermal image. This is the best method for extracting image corners. After Thermogram someone took pictures from a patient, the image must be converted to gray image format using an appropriate threshold, So we can, the main organ extract from image by using of active contour for later analysis. Otsu's technique is adopted to obtain the optimal level of threshold in order to minimize the intra-class variance (29). Detection of corners has been used in many aspects of image processing and machine vision (Fig.1).

Fig. 1: Images obtained the method of edge detection

Finding all the corners, measure of the exact position of the corner and robustness of algorithm against noise is resistant to noise, are important in edge detection. By using specific characteristics, simpler picture of the structure of image could be obtained in which important information of image is displayed. The corner is one of the special features widely used in the analysis of sense**.** Some of the important criteria for detection of corner includes**:** a) all corners should be detected; b) Anything wrong corner is not found; c) corners should be evident in their exact position; F) The corner detector should be robust against noise (30-33). Methods of corner detection including the Curvature, model of corner, peripheral curve. In this paper, using methods based on scale space, the corner position is extracted**.** Scale space allows the edges of the space with carefully down the space with high accuracy to be examined**.** This work is done by applying the Gaussian filter with different standard deviation (34). K is calculated by the following equation (35):

$$k(u,\sigma) = \frac{\dot{X}(u,\sigma)\ddot{Y}(u,\sigma) - \ddot{X}(u,\sigma)\dot{Y}(u,\sigma)}{(\dot{X}(u,\sigma)^2 + \dot{Y}(u,\sigma)^2)^{1.5}} \quad [1]$$

Where:

$$\dot{X}(u,\sigma) = x(u) \otimes \dot{g}(u,\sigma) \quad [2]$$

$$\ddot{X}(u,\sigma) = x(u) \otimes \ddot{g}(u,\sigma)$$

$$\dot{Y}(u,\sigma) = y(u) \otimes \dot{g}(u,\sigma)$$

$$\ddot{Y}(u,\sigma) = y(u) \otimes \ddot{g}(u,\sigma)$$

And $\otimes$ is the convolution operator, $g(u,\sigma)$ is Gaussian function with standard deviation σ,$\dot{g}(u,\sigma)$, $\ddot{g}(u,\sigma)$ are the first and second derivatives of the Gaussian function respectively. The original algorithms of css are used the following for detecting corner points of an image:

1. Canny edge detector is applied on the image gray levels and a binary edge map obtained.
2. Perimeter of edges is extracted from the map of edge, and distances between places are replenished, T connections are found.
3. The curvature in a large scale (σ_{high}), is calculated for the environment of each edge.
4. Local maximum points are selected as the point's initial corner points. The absolute size of curvature related to points must be higher than national threshold t and twice as one of local minimum of its neighbors.

5. Following corner points are applied in the largest scale to the smallest scale for improving their posture.
6. Comparison of T-fitting with the other corner and deletion of one corner points that is too close.

The scale-related algorithm has been used for finding the corner points and from multi- scale for establishing the corner points. Among corner points of candidate, although some are a local maximum, but most of them will be removed with the help of the local threshold.

The Endowment threshold is as follows:

$$T(u) = C \times \overline{K} = C \frac{1}{L_1+L_2+1} \sum_{i=u-L_2}^{u+L_1} K(i) \quad [3]$$

The average value of $\overline{k}$, was used to display average curvature of covered area of ROS. This area is defined as the minimum of the local curvature adjacent to the next. In general, a good corner must have been the desired angle, in order to be in a specific range. This angle (c_i) can be obtained from the following equation:

$$\angle C_i \left| \tan^{-1} \frac{\Delta Y_1}{\Delta X_1} - \tan^{-1} \frac{\Delta Y_2}{\Delta X_2} \right| \quad [4]$$

In which:

$$\Delta X_1 = \frac{1}{L_1} \sum_{i=u+1}^{u+L_1} X(i) - X(u) \quad [5]$$

$$\Delta Y_1 = \frac{1}{L_1} \sum_{i=u+1}^{u+L_1} Y(i) - Y(u)$$

$$\Delta X_2 = \frac{1}{L_2} \sum_{i=u-L_2}^{u-1} X(i) - X(u)$$

$$\Delta Y_2 = \frac{1}{L_2} \sum_{i=u-L_2}^{u-1} Y(i) - Y(u)$$

After this step, the set of candidate points is changed**;** several iterations must be done for converting the points. Using this criterion, segmented corner points may be removed due to noise and edgy detail and feature points of several sizes remain (Fig. 2).

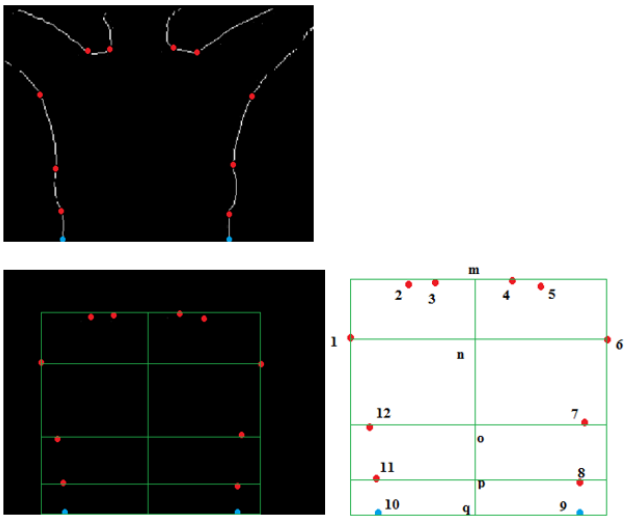

Fig. 2: Finding the main points in the thermal image

Coordinate of a point 9 and 10 are maximum points in image of edge detection. Coordinates of the point's m, n, o, p, q can be calculated by the following equations.

$$y_m = \frac{y_4 - y_3}{2} + y_3 \, , x_m \cong x_4 \quad [6]$$

$$y_n = \frac{y_6 - y_1}{2} + y_1 \, , x_n \cong x_6$$

$$y_o = \frac{y_7 - y_{12}}{2} + y_{12} \, , x_o \cong x_7$$

$$y_p = \frac{y_8 - y_{11}}{2} + y_{11} \, , x_p \cong x_8$$

$$y_q = \frac{y_9 - y_{10}}{2} + y_{10} \, , x_q \cong x_9$$

Currently methods used for feature extraction in thermal images for analysis, include geometrical features and wavelet moment (36-41). To be able to extract features that are resistant to the angle and rotation, the proposed method has been used which combines SURF and CORNER. Initial features are extracted using surf and corner algorithm. The first step is finding the key point. Our proposal is to use SURF descriptor, this descriptor is an extended form of sift, and much more (about 10 times) is faster than SIFT algorithm. SIFT algorithm can calculate the gradient of any area in the size 16 x 16 , then it is normalized , while the SURF algorithm is used by estimating the second order derivative of Gaussian function**,**convolved in image(42). Moreover instead of using time con-

suming calculations of sift, quick estimate, is used. Although SURF and SIFT have their advantages and disadvantages, But SURF algorithm works based on estimating the gradient of image pixels. Although the nature of the pixels change slightly (due to convolution of Gaussian function), it is desirable in other words, the pixel values remain constant (43,44). Sift makes the pyramids of the image for finding the candidate points makes, each layer filters Gauss law with increasing values of sigma and its acquired differences. On the other hand, surf makes use from hessian's matrix for selecting the candidate points with different sizes, as it is used in the hessian Laplace. Dominant angle over feature descriptor vector is obtained, using HAAR-wavelet filters and employing the integral image. Finally, using HAAR-wavelet filters is obtained a feature vector (44). Implementation steps of surf algorithm are shown on thermal images (Fig .3).

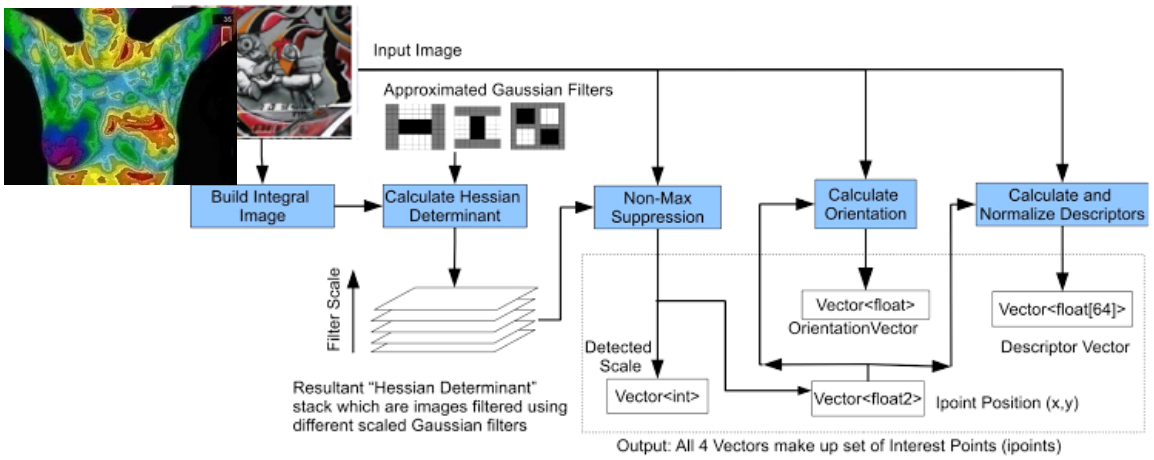

Fig. 3: Feature extraction by using surf algorithm

Totally, SURF utilizes a hessian based blob detector to find interest points. The determinant of a hessian matrix expresses the extent of the response and is an expression of the local change around the area (45). The heart of the SURF detection is non-maximal-suppression of the determinants of the hessian matrices**.**By determining a unique orientation for an interest point; it is possible to achieve rotational invariance. Finally, the descriptor is normalized, to achieve invariance to contrast those variations that will represent themselves as a linear scaling of the descriptor. The focused points extracted by surf algorithm are shown in Fig. 4.

Asmyd's assessment of the key point's detectors (46) shows that although Harris's detector, is not robust enough to changes scale, it has superior performance compared to the rest of detectors.

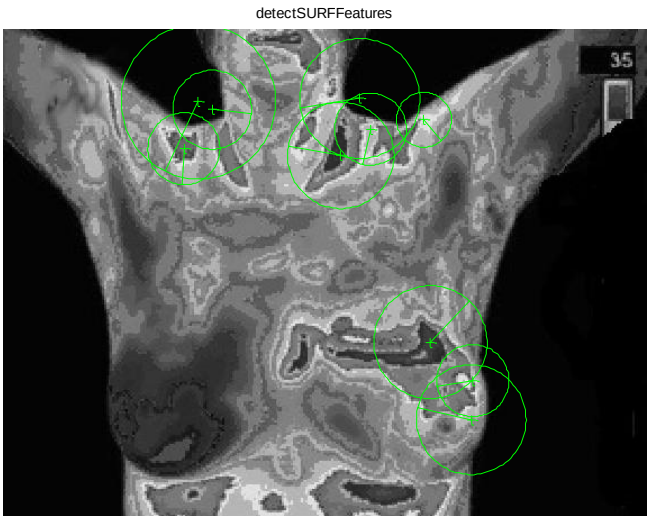

Fig. 4: The interest points detected in the infrared image

Harris's detector operates based on the second moment matrix. The second moment matrix is

used often for detection of features or to describe the internal structure of the image. This matrix must be adjusted to changes in scale, so it makes in depend of the accuracy and picture clarity. The second moment matrix is defined as follows (47):

$$\mu(X,\sigma_I,\sigma_D) = \begin{bmatrix}\mu_{11} & \mu_{12}\\ \mu_{21} & \mu_{22}\end{bmatrix} \text{ [7]}$$

$$=\sigma_D^2 g(\sigma_I) \times \begin{bmatrix} L_x^2(X,\sigma_D) & L_xL_y(X,\sigma_D)\\ L_xL_y(X,\sigma_D) & L_y^2(X,\sigma_D)\end{bmatrix}$$

σ is integrated scale,σ_D is differenced scale. This matrix describes the gradient distribution in the neighborhood of the point. The local derivatives are calculated using the Gaussian kernel (σ_D). Then the derivative is made average in the vicinity of point by smoothing with Gaussian window to the size σ_I.

Eigen values of this matrix show the variation of the two signals in the neighborhood of a point**.**Larger value of this feature indicates that its Point is high in both Major curve (Such as corners, connector locations, etc.).These points are sustainable in the favorable light conditions. Harris's detector is one of the most reliable detectors of the key points. Harris combines trace and Second moment matrix determinant in the following form (48)**:**

$$R = \det(\mu(X,\sigma_1,\sigma_D)) - \alpha \times trace^2(\mu(X,\sigma_1,\sigma_D)) \text{ [8]}$$

Local maximum of Harris (R) makes clear the location of the critical point. Harris detector is stable even in the presence of light that can provide same points. Also, Harris's detector can reveal the same points even when there are changes in the angle of view (48, 49).The output of the Harris's algorithm is shown in Fig. 5.

In the next step, points of interest identified by the surf and corner algorithm, combined and then used to segment cancerous tissue. Features Obtained from the surf and the corner are very important. However, it is possible that some parts of the features obtained from the corner method, are not important.

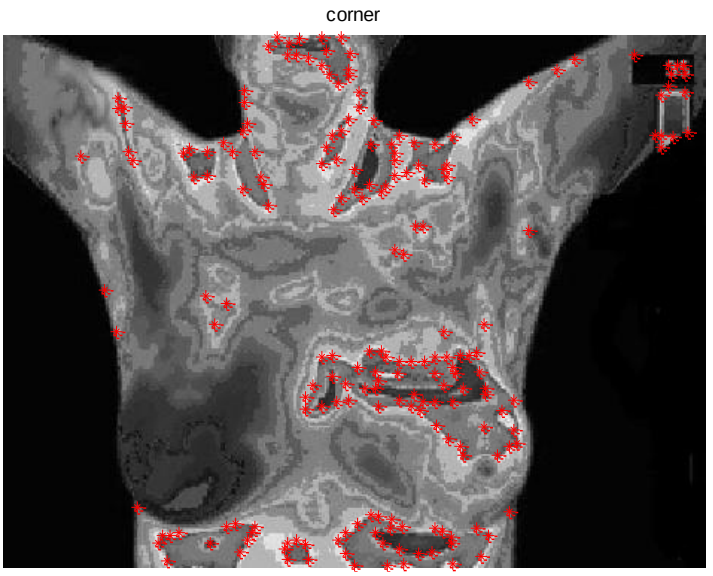

Fig. 5: Detected points by a Harris's method

So in the proposed method it is needed that the extracted features are combined together and used in both methods (SURF and SIFT). Initially extracted skeleton is partitionedand thenextracted features from the two methods are combined (Fig. 6).

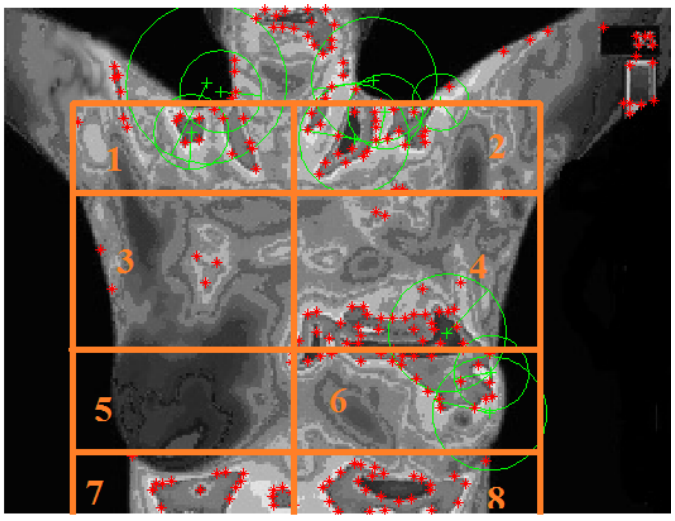

Fig. 6: Features combination of surf and sift algorithm

As shown in Fig. 6, Areas 4 and 6 needs to be reviewed, because breast cancer is noticeable in 3, 4, 5 and 6 districts. In addition, because areas 4, 6 are common so next focus will be on this area.

The next step requires that the cancerous cancer be segmented from image, done using active contour methods. Active contour models are powerful tools for identifying and tracking images, used extensively in applications of machine vision and image processing. Object detection with the help of active contour models is done based on tracking the boundaries of the target object. In this method, the contour curve is defined by the user or automatically around the target object, used from the extracted features for contour curves in this paper. Then this contour is deformed effected by the energy function, to be adapted with boundaries of target object (50, 51) . Active contour models have been used for the sake of segmenting. Active contour model is a parametric curve in the screen, as follows:

$$s(u) = I\big(x(u), y(u)\big) \quad u = [0,1] \quad [9]$$

This curve is transformed under the influence of an energy function, and is guided towards the features of interest in an image. Points of contour moves in the space coordinates (x, y), as long as curve is coincided to the favorite features of the desired object. The energy function is defined as follows (52-53):

$$E = \int_0^1 E_{snake}\big(S(u)\big)du \quad [10]$$

Which includes the internal energy and the energy of the image:

$$E = \int_0^1 E_{int}\big(S(u)\big) + E_{img}\,(S(u))du \quad [11]$$

It is best boundaries for contour, which has the lowest energy (Fig. 7), so finding the boundary of the object, is equivalent to minimizing the energy function of contour.

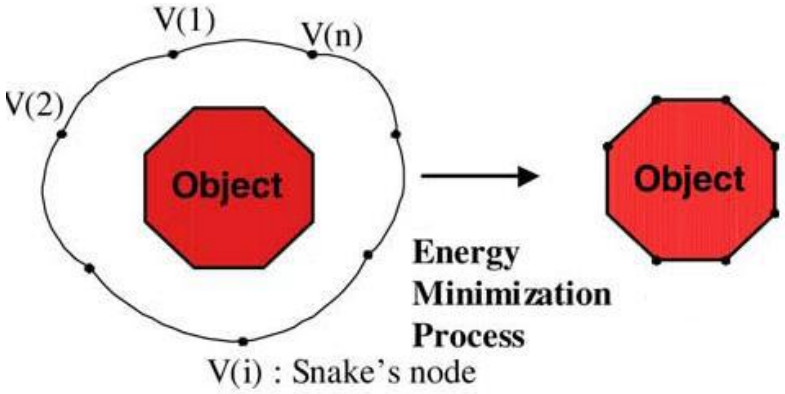

Fig. 7: Segmentation by using a parametric active contour model (54)

In which internal energy depends on the internal features of the contour such as elasticity rate and curvature, calculated as follows:

$$\mathrm{E_{int}} = \frac{\alpha}{2}\left|\frac{\partial}{\partial \mathrm{u}}\mathrm{S(u)}\right|^2 du + \frac{\beta}{2}\left|\frac{\partial^2}{\partial \mathrm{u}^2}\mathrm{S(u)}\right|^2 du \quad [12]$$

The first part of the internal energy causes the contour, act like a spring in order to determine the elastic curve. The second part determines the internal energy curve of the rate of resistance against bending. In the above equation, the coefficients α, β are weighted, which control sensitivity rate of counter against stretching and bending. Energy of image, direct the contour curves to the favorite features and distinct image such as edges, lines, corners and etc. and is calculated as follows (52):

$$\mathrm{E_{img}} = E_{edge} = -p|\nabla I(s)|^2 \quad [13]$$

Parameter p is a huge amount of image energy, ∇ indicates the gradient operator. Hence, the total energy of the active contour is defined as follows:

$$E = \frac{\alpha}{2}\oint \left|\frac{\partial}{\partial u}S(u)\right|^2 du + \frac{\beta}{2}\oint \left|\frac{\partial^2}{\partial u^2}S(u)\right|^2 du + \oint \mathrm{E_{edge}}\big(\mathrm{S(u)}\big)\mathrm{du} \quad [14]$$

If there is a visual prominent feature (strong edge), energy function guides the contour curve towards the target correctly. Unfortunately in the absence of strong edges, curve of contour becomes diffi-

cult to find the target object. For overcoming this problem, the new energy has been used called the Strain energy of color, and is replaced by edge energy in equation 7(55-57).This energy produces a compressive force, and contour is condensed toward the target object (or is expanded). The Pressure energy of color can be defined as following:

$$E_{pressure} = p\, G(I(s))\left(\frac{\partial S}{\partial u}\right)^{\perp} \quad [15]$$

Where P is a parameter that determines the magnitude of the pressure energy and is loaded by the user. G is a function, in accordance with Equation 18 as (56):

$$G\big(I(s)\big) = \begin{cases} +1 \;\; if\; I \geq T \\ -1 \;\; otherwise \end{cases} \quad [16]$$

T is the intensity threshold of image**.**Considering that most features are in the district 4, therefore the initial active contour should be created in the district 4. The final frontier of active contour, as can be seen in Fig. 8, is controlled by the corners. Now we can apply the proposed contour on the image. Fig. 9 shows the proposed contour after 100, 130, 200 and 250 iterations.

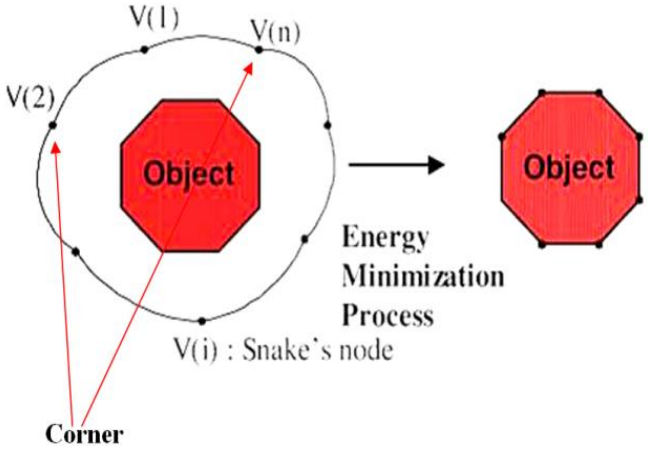

Fig. 8: Adaptation of surf & sift algorithm with active contour

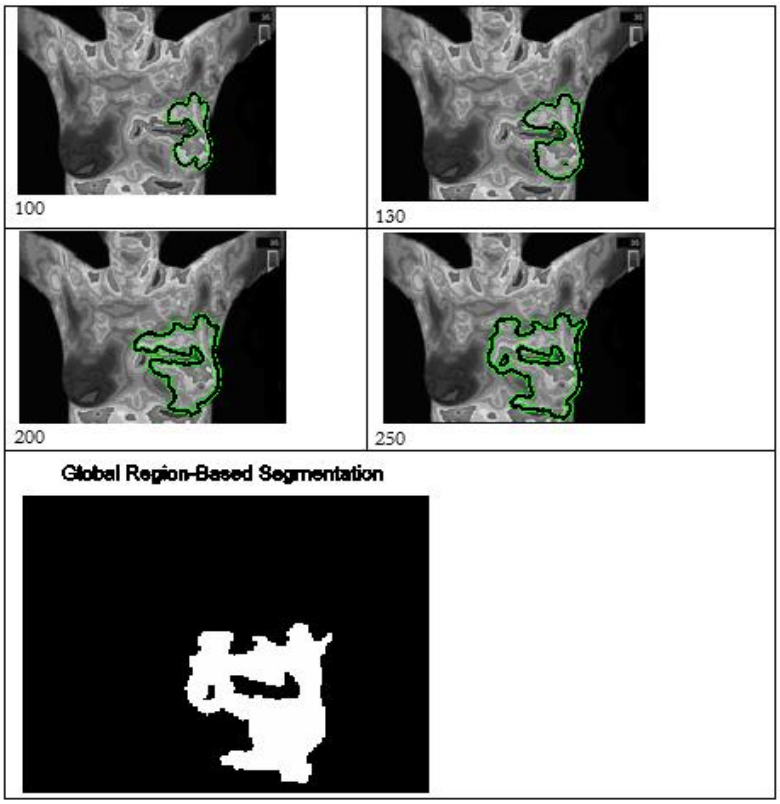

Fig. 9: Implementation of active contours in steps 100, 130, 200, 250 and Extraction of the cancerous area from the thermal image

As can be seen in Fig. 9 cancerous tissue has been segmented from the image accurately and suitably. The proposed method enables us to diagnose the structure of the isolated tissue. The detection is performed using Lyapunov exponent test model**.**By this test it is possible to distinguish accidental from non-accidental time series without statistical distribution. We can express the similarity of data in a time series, so that period of effect data appears to predict the future. This test is described as follows. Suppose we have N observation of a chaotic time series available as follows: X_i, i= 1,2,…, N [17]

In this case, to obtain the Lyapunov exponent, divided M vectors is initially formed from these time series as follows:

X_I^M= (Xi, Xi+1,... , Xi+M−1) ; i = 1,2,..., N −M +1 [18]

Then among these vectors, all pairs of vectors proved in the following equation, Are determined:

$$r_0(M;i,j) = \left|X_i^M - X_j^M\right| \le r \quad [19]$$

Where r is a small positive number and $\|.\|$ is the 2-norm, which indicates the distance in Euclidean space. Now with transfer time to the n-step ahead, this distance is computed again, thus:

$$d_n(M;i,j) = \frac{r_n(M;i,j)}{r_0(M;i,j)} = \frac{\left\|X_{i+n}^M - X_{j+n}^M\right\|}{\left\|X_i^M - X_j^M\right\|} \quad [20]$$

If these vectors are far apart we result that d_n is the larger than one Otherwise, smaller than 1. Thus, the largest Lyapunov exponent is calculated as follows:

$$L(M,n) = \sum_{i\neq j} \frac{log\,[d_n(M;i,j)]}{N(N-1)} \quad [21]$$

The positive value of L indicates that time series is chaotic and predicted in divergent way. The negative value of L represents a definitive nature for time series and Long-term predictability. So if L accepts positive values close to zero, the system are weakly chaotic and medium-term prediction is possible, but predicted long-term is impossible. Up to now, following steps are done using original image. First distance of center related to the segmented area from it edge is calculated as time series and distance values are written in the same way, Then Lyapunov exponent test is employed. Now by using a test, we can identify the type of tissue.

Results

In this section, the results of the proposed method are compared with mammography results. Assessed Images are from 20 cancerous patients (Fig. 10).

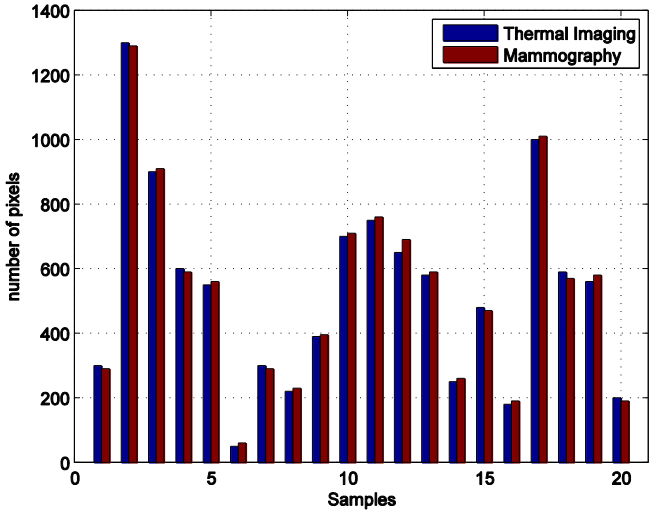

Fig. 10: Bar Chart on pixel area traced by radiologist versus balloon snake

For validating the overall performance of the proposed method, the breast tumor regions obtained by the proposed method were compared with those plotted by the radiologist. Three error metrics were defined: the true-positive ratio (TP), the false-positive ratio (FP) and the false-negative ratio (FN) (60). Let A_a be the pixel set of the ROIs determined by the proposed method and Am be the pixel set of the ROIs determined manually by the radiologist; the three error metrics are calculated as:

$$TP = \frac{|A_m \cap A_a|}{|A_m|} \quad FP = \frac{|A_m \cup A_a - A_m|}{|A_m|} \quad FN = \frac{|A_m \cup A_a - A_a|}{|A_m|} \qquad [22]$$

When the TP ratio is higher and the FN ratio is lower, more real tumor regions are classified as "breast lesion" regions, and when the FP ratio is lower, fewer normal tissue regions are classified as "breast lesion" regions. Values obtained include TP= 91.31%, FN=8.69%, FP=7.26%.Lyapunov exponent for the segmented areas results that the rate of chaos for benign case is much less than the malignant cases. In another words, the boundaries of benign case is smoother than the malignant case (Fig. 11).

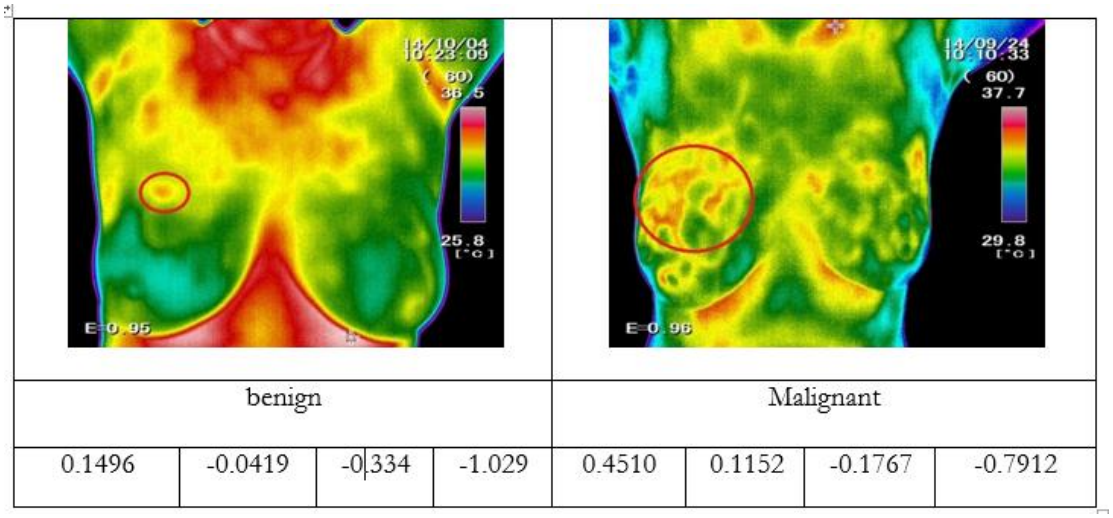

Fig.11: The obtained value for Lyapunov exponent in the images related to breast cancer

Discussion

Mammography is the most common method of breast imaging. Cancerous masses and calcium deposits appear brighter on the mammogram. Mammography can be considered as the golden standard method for breast cancer detection. Applying mammographic screening is very difficult to detect cancer in the very early stages. Additional screening methods such as the use of Thermograms may help lower the death rate from the breast cancer. Cancerous and pre-cancerous tissues have a higher metabolic rate resulting in the growth of new blood vessels to supply nutrients to the cancerous cells. Consequently, the temperature of the tissue surrounding the pre-cancerous tissue is higher than the other regions. Hence, pre-cancerous and cancerous tissues appear as hot spots in breast thermal images. Breast Thermography is a method providing images of breast thermal patterns. Mammography detects anatomical changes while Thermography detects physiological changes that occur much earlier than anatomical changes. A combination of mammography and Thermography methods can perform better in detecting invasive cancer and multifocal diseases. The keys to obtaining higher accuracy would be (a) high sensitivity imaging to obtain reliable hot spot information related to metabolic activity in the breast, (b) to process Thermogram to isolate these regions from the background, (c) to use a feature extraction algorithm such as the

one described here that will capture information about the spatial distribution of these regions while being robust to translation and scale changes and (d) to use a good feature selection, fusion and classification algorithm such as Ad boost. The Features extracted from a collection of images can be used for training and clustering of systems. Many previous studies have used only the difference in temperature between the affected area and normal (asymmetric techniques), for breast cancer detection. Some researchers have suggested that "distribution" of the actual temperature difference between the thermal image and temperature data normalization (ideally) is a better way to detect cancerous areas (58). Recently, intelligent computers that have features such the support of multimedia and data-mining have assisted the radiologist (59).

Conclusions

Although breast cancer is not a new disease**,** it has been increased in women to an unprecedented level in the world in recent decades. If it is diagnosed early, it can be treated easily. In previous research, many methods have been proposed to form a mathematical model for pattern classification. In this paper, we presented a method of completely automatic segmentation that can diagnose the breast cancer core in the breast thermal images. This paper drew one combination model of feature extraction related to surf and corner algorithm that are robust. Finally, extracted features are used for detecting breast cancer based on active contour. The proposed model for active contour is able to segment cancerous areas accurately. Experiments show that the proposed method can be reliable and useful**.** The proposed method can solve problems created in imaging. These problems include undesirable quality of image and cancerous areas segmentation.

Ethical considerations

Ethical issues (Including plagiarism, informed consent, misconduct, data fabrication and/or falsification, double publication and/or submission, redundancy, etc.) have been completely observed by the authors.

Acknowledgement

The authors declare that there is no conflict of interests.

Reference

1. National Cancer Institute (2012). Seer stat fact sheets: female Breast cancer. Available from: http://www.seer.cancer.gov/statfacts/html/breast.html.
2. Ng EYK, Sudarshan NM (2001). Numerical computation as a tool to aid thermo graphic Interpretation. *J Med Eng Technol*, 25(2):53–60.
3. Leung TK, Lee CM, Chen CH et al (2009). Far infrared ray irradiation induces intracellular generation of nitric oxide in breast cancer cells. *J Med Boil Eng*, 29(1):15-18.
4. Kerr J (2004). Review of the effectiveness of infrared thermal imaging (thermography) for population screening and diagnostic testing of breast cancer. *NZHTA Tech Brief Series,* 2004; 3(3).
5. Huang CL, Wu YW, Hwang CL, et al (2011). The application of infrared thermography in evaluation of patients at high risk for lower extremity peripheral arterial disease. *J Vasc Surg*, 54(4):1074-1080.
6. Ring EFJ, Ammer K (2012). Infrared thermal imaging in medicine. *Physiol meas,* 33(3):R33-46.
7. Ng EYK (2008). A reviews of thermography as promising non-invasive detection modality for breast tumor. *Int J Therm Sci*, 48:849-855.
8. Tan JH, Ng EYK, AcharyaU R, Chee C (2009).Infrared Thermography on ocular surface temperature: a review. *Infrared Phys Techn*, 52:97-108.
9. Ng EYK, Kee EC (2007). Advanced integrated technique in breast cancer Thermography. *J Med Eng Technol*, 32(2):103-114.
10. Ng WK, Ng EYK, Tan YK (2009). Qualitative study of sexual functioning in couple with ED: prospective evaluation of the Thermography diagnostic system. *J Reprod Med*, 54(11-12): 698-705.

11. Ng EYK, Kaw GJL, Chang WM (2004). Analysis of IR thermal imager for mass blind fever screening. *Microvasc Res*, 68(2): 104-109.
12. Francis SV, Sasikala, M, Bharathi GB, Jaipurkar SD (2014). Breast cancer detection in rotational thermography images using texture features. *Infrared Phys Techn*, 67:490-496.
13. Arora N, Martins D, Ruggerio D, Tousimis E, Simmons M at al (2008). Effectiveness of a noninvasive digital infrared thermal imaging system in the detection of breast cancer. *Am J Surg*, 196(4): 523–526.
14. Arabia P, Muttan S (2012). Multiple Irradiations by Hybrid Source for Early Breast Carcinoma detection. *Procedia Eng*, 38: 2398–2412.
15. Wang S (2003). An Observation on Infrared Thermograph of Lower Back Pain Patients. *Ind Health Occ Dis*, 29(1).
16. Cheng KS, Yang SJ, Wang MS, Pan SC (2002). The application of thermal image analysis to diabetic foot diagnosis. *J Med Biol Eng*, 22(2):75–82.
17. Duarte A, Carrão L, Espanha M, Viana T, Freitas D, Bártolo P, Almeida H.A (2014). Segmentation algorithms for thermal images. *Procedia Technol*, 16: 1560-1569.
18. Mabuchi K, Chinzei T at al (1998). Evaluating asymmetrical thermal distributions through image processing. *IEEE Eng Med Biol Mag*, 17(4): 47–55.
19. Fujimasa I (1998). Path physiological expression and analysis of far infrared thermal Images-A standard thermo graphic image diagnosis procedure using computed image processing. *IEEE Eng Med Biol*: 34–42.
20. RajendraAcharya U, Ng EYK, Tan JH, VinithaSree S (2012). Thermography Based Breast Cancer Detection Using Texture Features and Support Vector Machine. *J Med Syst,* 36(3):1503-1510.
21. Hairong Qi, Kuruganti PT (2002). *Detecting Breast Cancer from Thermal Infrared Images by Asymmetry Analysis*. Eds, Medical Devices and Systems.1st ed, Joseph Bronzino. New York, pp.1155-1186.
22. Eng H, Thida M, Chew B, Leman K, Anggrelly S (2008). Model -based detection and segmentation of vehicles for intelligent transportation system. *IEEE Conf Ind Elec Appl,* 2127-2132.
23. Huang K, Tan T (2010). Vs-star: a visual interpretation system for visual surveillance. *Pattern Recogn Lett*, 31(14):2265-2285.
24. Harandi N, Sadri S, Moghaddam N, Fattahi R (2010). An automated method for segmentation of epithelial cervical cells in images of thin Prep. *J Med Syst*, 34(6):1043-1058.
25. Chen Q, Sun Q, Heng P (2010). Two - stage object tracking method based on kernel and active contour. *IEEE T Circ Syst Vid*, 20(4): 605-609.
26. Jumaat A, Rahman We, Ibrahim A, Mahmud R (2010). Segmentation of Masses from Breast Ultrasound Images using Parametric Active Contour Algorithm. *Procedia Social Behav Sci,* 8:640–647.
27. Lee J, Muralidhar GS, Reece GP, Markey MK (2012). A shape constrained parametric active contour model for breast contour detection. *Conf Proc IEEE Eng Med Biol Soc,* 2012;2012:4450-4453.
28. EtehadTavakol M, Ng EYK, Lucas C, Sadri S, Ataei M (2012). Nonlinear analysis using Lyapunov exponents in breast thermograms to identify abnormal lesions. *Infrared Phys Techn*, 55(4):345–352 ·
29. Sahoo P, Wilkins C, Yeager J (1997). Threshold selection using Renyi's entropy. *Pattern recognit,* 30(1):71-84.
30. Lesser VR, Nawab SH, Klassner FI (1995). IPUS: architecture for the integrated processing and understanding of signals. *Artif Int*, 77(1):129-171.
31. Mokhtarian F, Mohanna F (2006). Performance evaluation of corner detectors using consistency and accuracy measures. *Comput Vis Image Und*, 102(1):81-94.
32. Shen F, Wang H (2000). Real time gray level corner detector. *Conf Rob Vision,* 6:1-4.
33. GoutamMajumder G, Bhowmik MK, Bhatacharjee D (2013). Automatic Eye Detection Using Fast Corner Detector of North East Indian (NEI) Face Images. *Procedia Technol,* 10: 646–653.
34. Olson C.F (2000). Adaptive-scale is filtering and feature detection using range data. *IEEE T Pattern Anal,* 22(9):983-991.
35. Zhang X,Lei M, Yang D, Wang Y,Ma L (2007). Multi-scale curvature product for robust image corner detection in curvature scale space. *Pattern Recogn Lett,* 28(5):545-554.

36. Junli H (2004). Research for Target Recognition of Infrared Bridge Based on Morphological Operator and Bridge Template. *IEEE Comput Sci*, 58-62.
37. Jinle Z, Yirong Z, Dong D, Baohua C, Jiluan P (2015). Research on a visual weld detection method based on invariant moment features. *Ind Rob Int J*, 42(2):117-128.
38. Bing X (2007). Research of image's scale and rotation invariant recognition based on invariant moment. *Shanxi,* 1:19-26.
39. Wong Y.R (1978). Scene Matching With Invariant Moment. *Comput Graphics Image Process, 8(1):16-24*.
40. Dong CH, Yongjie H, Zhenkang SH (2001). Research of feature extraction method of infrared image based on scale singular value transforms. *Infrared Laser Eng*, 6:157-159.
41. Zhongcheng ZH, Qinghua M, Zhen Kang SH (1999). Feature analysis of infrared target. *Laser Infrared*, 6:166-169.
42. Chao-jian X, San-xue G (2011). Image target identification of UAV based on SIFT. *Procedia Eng*, 15: 3205-3209.
43. Bradski G, Kaehler A (2008). *Learning OpenCV: Computer vision with the Open CV library*. 3rd ed. Reilly Media, Canasa, pp.100-110.
44. Herbert B, Ess A, Tuytelaars T, Gool LV (2008). SURF: Speeded Up Robust Features. *Comput Vis Image Und*, 110(3): 346-359.
45. Wikipedia (2011). Blob detection. Available from: https://en.wikipedia.org/wiki/Blob_detection .
46. Mikolajczyk K, Schmid C (2005). A performance evaluation of local descriptors. *IEEE Conf Comput Vision,* 27(10):1615-1630.
47. Baumberg A (2000). Reliable feature matching across widely separated views. *IEEE Conf Comput Vision,* 1:774–781.
48. Sroba L, Ravas R, Grman J (2015). The Influence of Sub pixel Corner Detection to Determine the Camera Displacement. *Procedia Eng*, 100:834-840.
49. Alexandre A, Raphael O, Vandergheynst P (2012). FREAK: Fast Retina Key point. *IEEE Conf Comput Vision*, 1:16-21.
50. Charoensa kC (2004). Face contour tracking in video using active contour model. In Image Processing. *IEEE Image Process,* 2:1021-1024.
51. Fu Y, Erdem T, TekalpA M (2000). Tracking visible boundary of objects using occlusion adaptive motion snake. *IEEE Trans Image Process*, 9(12):2051–2060.
52. Kass M, Witkin A, Terzopoulos D (1988). Snakes: active contour models. *Int Conf Comput Vis,* 321-331.
53. Prince JL, Xu C (1996).A new external force model for snakes. *In Image Multidimension Signal Process Workshop,* 30–31.
54. Kim W, Lee J (2005). Object tracking based on the modular active shape model. *Mechatronics*, 15(3):371-402.
55. Ivins J, Porrill J (1994). Active region models for segmenting medical images. *IEEE Int Conf Image Process*, 2: 227-231.
56. Hamarneh G, Chodorowski A, Gustavsson T (2000). Active Contour Models: Application to Oral Lesion Detection in Color Images. *IEEE Int Conf Syst*, 4: 2458 -2463.
57. Schaub H, Smith C (2003). Color snakes for dynamic lighting conditions on mobile manipulation platforms. *IEEE Int Conf Intel Rob Syst*, 2:1272-1277.
58. Mabuchi K, Chinzei T, Fujimasa I, Yonezawa T at al(1997). An image-processing program for the evaluation of asymmetrical thermal distributions. *IEEE Eng Med Biol Soc*, 2:725-728.
59. Perner P (2000). Mining knowledge in medical image databases, in: Belur V. Dasarathy (Ed.), Qerner Proceedings of SPIE - Data Mining and Knowledge Discovery: Theory. *Tools Technol,* 4057: 359–369.
60. Madabhushi A, Metaxas DN (2003). Combining low-, high-level and empirical domain knowledge for automated segmentation of ultrasonic breast lesions. *IEEE Trans Med Imaging*, 22(2):155–169.